JOC Article
pubs.acs.org/joc

Understanding the Electronic Reorganization along the Nonpolar [3 + 2] Cycloaddition Reactions of Carbonyl Ylides.

Luis R. Domingo* and José A. Sáez

Departamento de Química Orgánica, Universidad de Valencia, Dr. Moliner 50, E-46100 Burjassot, Valencia, Spain

domingo@utopia.uv.es

Received July 14, 2010

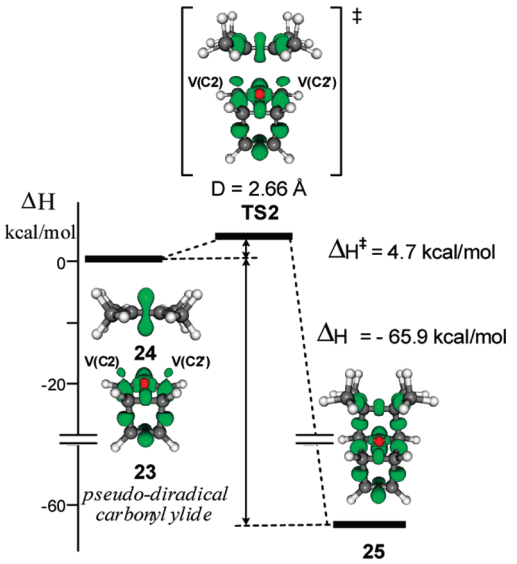

The nonpolar [3+2] cycloaddition (32CA) reaction of the carbonyl ylide (CY) **23** with tetramethylethylene (TME) **24** has been studied with DFT methods at the B3LYP/6-31G* level. This cycloaddition reaction, which has a very low activation energy of 4.7 kcal/mol, takes place through a synchronous transition structure. A topological analysis of the ELF along the 32CA reaction provides a new scope of the electronic structure of CY **23** as a pseudodiradical species offering a sound explanation of the high reactivity of this CY in nonpolar reactions. In addition, this analysis points to the nonparticipation of the oxygen lone pairs in the 32CA reaction. This cycloaddition can be seen as a pseudodiradical attack of the terminal carbon atoms of the CY **23** on the π system of TME **24**. Therefore, the present study establishes that this 32CA reaction, which is not a pericyclic electron reorganization, may be electronically classified as a [2n + 2π] process.

1. Introduction

Cycloaddition reactions are among the most useful organic reactions in the toolbox of the synthetic organic chemist because of their ability to create regio- and/or stereoselectively cyclic motifs with organic molecules.[1] Classified as cycloaddition processes, Diels−Alder (DA) reactions have been found to present predictable mechanisms: the increase of the charge transfer (CT) between both reagents, the diene and the dienophile, at the transition state (TS) structure decreases the activation energy associated with the reaction (see reactions a and b in Scheme 1).[2]

Unlike DA reactions, [3 + 2] cycloaddition (32CA) reactions lack a clear systematization of their reactivity based on the

(1) (a) Wasserman, A. *Diels-Alder Reactions*; Elsevier Pub. Co.: New York, 1965. (b) Carruthers, W. *Cycloaddition Reactions in Organic Synthesis*; Pergamon: Oxford, UK, 1990. (c) Padwa, A. *1,3-Dipolar Cycloaddition Chemistry*; Wiley-Interscience: New York, 1984; Vols. 1−2. (d) Padwa, A. *Comprehensive Organic Chemistry*; Pergamon: Oxford, UK, 1991; Vol. 4.

(2) Domingo, L. R.; Sáez, J. A. *Org. Biomol. Chem.* **2009**, *7*, 3576–3583.

DOI: 10.1021/jo101367v Published on Web 12/15/2010

SCHEME 1

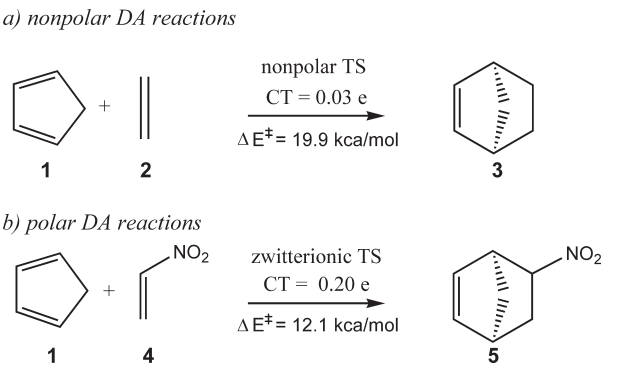

nucleophilic/electrophilic behavior of the reagents. Thus, the 32CA reaction between the fulminic acid **6** and ethylene **2**, which has a nonpolar character, presents a low activation energy, $\Delta E^{\ddagger} = 11.3$ kcal/mol (see Scheme 2),[3] which is only slightly reduced with the electronic activation of both reagents.[3c] A more drastic situation is found in the 32CA reactions of azomethine ylides (AY). In spite of the low reactivity of ethylene **2**, the 32CA reaction between the simplest AY **8** and ethylene **2** presents an unappreciable activation energy, $\Delta E^{\ddagger} = 1.2$ kcal/mol,[4] which is not modified by a nucleophilic activation of the AY **10** and the electrophilic activation of acrylonitrile **11** (see Scheme 2).[5]

To explain the high reactivity of the electronically nonactivated AYs in 32CA reactions, Domingo et al.[6] have recently performed a theoretical study of the electronic reorganization along the 32CA reaction of the AY **8** with ethylene **2** using the topological analysis of the electron localization function (ELF).[7] This study stressed that the pseudodiradical[8] character of the AY **8** is responsible for the high reactivity of this species. When analyzing the ELF of selected points along this concerted cycloaddition, it was found that only the two nonbonding electrons located at the terminal carbon atoms of the AY **8** and the two π electrons of ethylene **2** are involved in the 32CA reaction. This cycloaddition has been electronically classified as a [2n + 2π] process.[6]

SCHEME 2

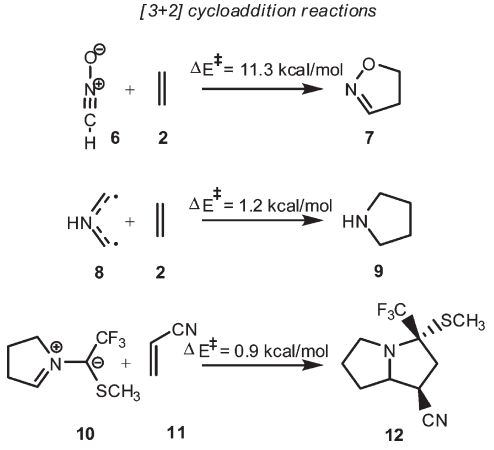

Recently, the 32CA reactions of carbonyl ylide (CY)[10] **13** and the Padwa's CY **16**,[11] which also present very low activation energies, were theoretically studied (see Scheme 3). For the electrophilically activated CY **13**, the most favorable channel was associated to the nucleophilic attack of the carbonyl oxygen atom of isatin **14** to CY **13**,[10] whereas for the nucleophilically activated CY **16**, the most favorable channel was characterized by the attack of the Padwa's CY **16** on the β-conjugated position of the α,β-unsaturated ketone **17**.[11] The behaviors of these CYs are in complete agreement with the high electrophilicity,[12] ω, and nucleophilicity,[13] N, indices showed by these CYs: $\omega = 4.29$ for **13** and $N = 4.50$ eV for **16**.

SCHEME 3

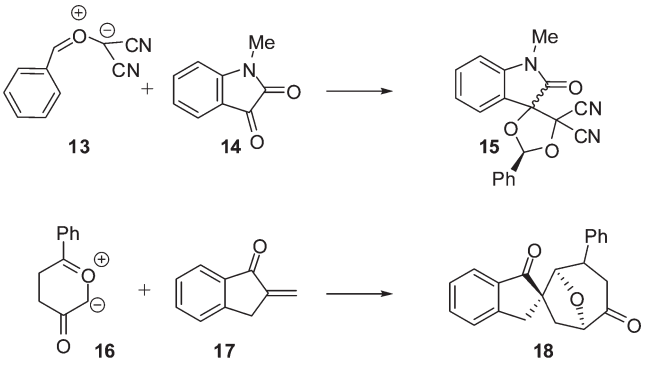

CYs derived from a thermal aperture of oxaquadricyclanes (OQC) may behave as the three-atom component in 32CA reactions. Recently, Szeimies et al. have performed an experimental and computational study on the mechanism of the thermal rearrangement of the OQC **19** to give the cage compound **21** (see Scheme 4).[14] The intramolecular 32CA reaction of the intermediate CY **20** presented also a very low activation energy (4.2 kcal/mol at UB3PW91/6-311G** and 3.6 kcal/mol at CASPT2(8,7)/6-31G*).[14] The CY **20**, with a $\langle s^2 \rangle = 0$, was represented as a zwitterionic structure.

(3) (a) Poppinger, D. *J. Am. Chem. Soc.* **1975**, *97*, 7486–7488. (b) Sosa, C.; Andzelm, J.; Lee, C. T.; Blake, J. F.; Chenard, B. L.; Butler, T. W. *Int. J. Quantum Chem.* **1994**, *49*, 511–526. (c) Domingo, L. R.; Chamorro, E.; Perez, P. *Eur. J. Org. Chem.* **2009**, 3036–3044.

(4) Alvarez, A.; Ochoa, E.; Verdecia, Y.; Suarez, M.; Sola, M.; Martin, N. *J. Org. Chem.* **2005**, *70*, 3256–3262.

(5) Domingo, L. R. *J. Org. Chem.* **1999**, *64*, 3922–3929.

(6) Domingo, L. R.; Chamorro, E.; Pérez, P. *Lett. Org. Chem.* **2010**, *7*, 432–439.

(7) (a) Savin, A.; Becke, A. D.; Flad, J.; Nesper, R.; Preuss, H.; Vonschnering, H. G. *Angew. Chem., Int. Ed.* **1991**, *30*, 409–412. (b) Savin, A.; Silvi, B.; Colonna, F. *Can. J. Chem.* **1996**, *74*, 1088–1096. (c) Savin, A.; Nesper, R.; Wengert, S.; Fassler, T. F. *Angew. Chem., Int. Ed. Engl.* **1997**, *36*, 1809–1832. (d) Silvi, B. *J. Mol. Struct.* **2002**, *614*, 3–10.

(8) In 1960 Errede et al. studied the high chemical reactivity of *p*-xylylene,[9] which was attributed to its pseudodiradical character. They defined a pseudodiradical as a diamagnetic compound that behaves chemically as if were a diradical. Errede, L. A.; Hoyt, J. M.; Gregorian, R. S. *J. Am. Chem. Soc.* **1960**, *53*, 5224–5227.

(9) *p*-Xylylene, which has a ground state quinoleine-like structure, has a B3LYP/6-31G* stable closed shell wave function. The triplet state, which has a benzene-like structure, is located 31.1 kcal/mol above ground state.

(10) (a) Bentabed-Ababsa, G.; Derdour, A.; Roisnel, T.; Sáez, J. A.; Domingo, L. R.; Mongin, F. *Org. Biomol. Chem.* **2008**, *6*, 3144–3157. (b) Bentabed-Ababsa, G.; Derdour, A.; Roisnel, T.; Sáez, J. A.; Pérez, P.; Chamorro, E.; Domingo, L. R.; Mongin, F. *J. Org. Chem.* **2009**, *74*, 2120–2133.

(11) Benchouk, W.; Mekelleche, S. M.; Aurell, M. J.; Domingo, L. R. *Tetrahedron* **2009**, *65*, 4644–4651.

(12) Parr, R. G.; von Szentpaly, L.; Liu, S. *J. Am. Chem. Soc.* **1999**, *121*, 1922–1924.

(13) Domingo, L. R.; Chamorro, E.; Pérez, P. *J. Org. Chem.* **2008**, *73*, 4615–4624.

(14) Glück-Walther, S.; Szeimies, G. *Helv. Chim. Acta* **2005**, *88*, 1540–1552.

SCHEME 4

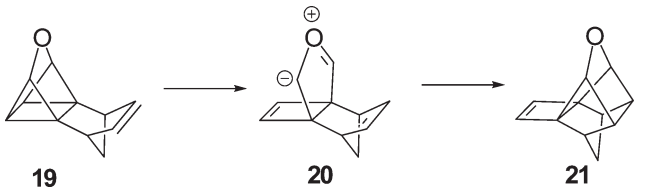

Very recently, Hiberty et al. have reported a correlation between the diradical character of some 1,3-dipoles, including AY **8**, and their reactivity toward ethylene **2** and acetylene.[15] They propose a mechanism for the 32CA reaction, in which the dipole first distorts so as to reach a reactive electronic state that has a significant diradical character, which then adds to the dipolarophile with little or no barrier. On the other hand, they note that the diradical character of the reactive state, albeit important, is still very far from that of a pure diradical state.[15] Therefore, they suggest that their results can in no way be interpreted as a support for a diradical mechanism being as good as a concerted reaction. Our recent study about the changes on bonding on the 32CA reaction between AY **8** with ethylene **2** have suggested that the pseudodiradical character of AY **8**, which remains at the TS, is responsible for the high reactivity of AYs in nonpolar processes.[6] This behavior is a consequence of the semblance between the electronic structure of the pseudodiradical AY **8** and the pseudodiradical species found at a distance of 2.15 Å on the IRC from the TS to the CA **9**, which is responsible for the formation of the two C−C bonds.[6]

In the present work, a density functional theory (DFT) study for the thermal reaction of OQC **22** with tetramethylethylene (TME) **24**, which has been experimentally studied,[16] is carried out in order to explain the high reactivity of nonactivated CYs on nonpolar 32CA reactions (see Scheme 5). A complete characterization of the electronic reorganization along the intermolecular 32CA reaction between the electronically nonactivated CY **23** and TME **24** is fulfilled. To do so, a topological analysis of the ELF of some selected points of the IRC along the reaction path associated to this 32CA reaction will be performed.

2. Computational Methods

All calculations were carried out with the Gaussian 03 suite of programs.[17] DFT calculations were carried out with the B3LYP[18] exchange-correlation functionals, together with the standard 6-31G(d) basis set.[19] The optimizations were carried out with the Berny analytical gradient optimization method.[20] The stationary points were characterized by frequency calculations in order to verify that TSs have one and only one imaginary frequency. The intrinsic reaction coordinate (IRC)[21] paths were traced in order to check the energy profiles connecting each TS

SCHEME 5

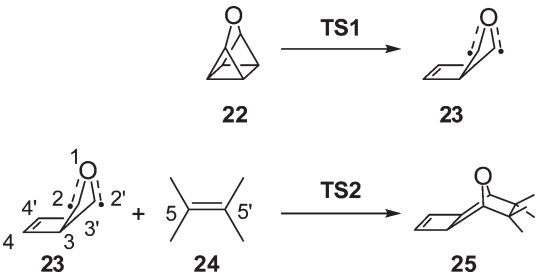

to the two associated minima of the proposed mechanism, using the second order González−Schlegel integration method.[22] The stationary points were also optimized by using the 6-311G(d,p) basis set.[19] The energy results are given in the Supporting Information. No significant changes in relative energies and geometries were found. The stability of the closed shell wave functions was checked with the STABLE = opt keyword. Only CY **23** presented instability. The UB3LYP/6-31G(d) open shell wave function, with $\langle s^2 \rangle = 0$, is only 0.6 kcal/mol more stable than the closed shell one. However, the closed shell wave function of **TS1** and **TS2** showed stability at both computational levels. Values of enthalpies, entropies, and free energies were calculated with the standard statistical thermodynamics at 353.15 K and 1 atm. In the thermodynamic calculations, harmonic vibrational frequencies were scaled by a factor of 0.96.[23] The electronic structures of stationary points were analyzed by the natural bond orbital (NBO) method[24] and by the topological analysis of the electron localization function (ELF), $\eta(\mathbf{r})$.[7] The ELF study was performed with the TopMod program[25] using the corresponding monodeterminantal wave functions of the selected structures of the IRC.

3. Results and Discussion

First, a mechanistic study of the thermal reaction between OQC **22** and TME **24** to yield the CA **25** will be made (Scheme 5). Then, an analysis of the geometrical and electronic structure of the CY **23** will be performed. Afterward, a detailed ELF study on the IRC path of the intermolecular 32CA reaction between the CY **23** and TME **24** will be carried out.

3.1. Mechanistic Study of the Thermal Reaction between OQC 22 and TME 24. The thermal 32CA reaction between the OQC **22** and TME **24** to yield the CA **25** is a domino process that comprises two consecutive reactions: (i) an intramolecular retro-32CA reaction at OQC **22** to yield the intermediate CY **23**, and (ii) an intermolecular 32CA reaction between CY **23** and TME **24** to yield the final CA **25**. To obtain mechanistic details of the formation of CA **25**, the two reactions involved in this domino process were studied by using DFT calculations at the B3LYP/6-31G* level (see Scheme 5).

In the gas phase, the activation enthalpy associated with the intramolecular retro-32CA at the OQC **22** via **TS1** to yield the CY **23** is 28.1 kcal/mol; this step is endothermic by 24.2 kcal/mol (see Table 1). These high unfavorable energies

(15) Braida, B.; Walter, C.; Engels, B.; Hiberty, P. C. *J. Am. Chem. Soc.* **2010**, *132*, 7631–7637.
(16) Prinzbach, H.; Babsch, H. *Angew. Chem., Int. Ed.* **1975**, *14*, 753–755.
(17) Frisch, M. J. *Gaussian03*, 2004; Gaussian, Inc., Wallingford, CT.
(18) (a) Becke, A. D. *J. Chem. Phys.* **1993**, *98*, 5648–5652. (b) Lee, C.; Yang, W.; Parr, R. G. *Phys. Rev. B* **1988**, *37*, 785–789.
(19) Hehre, W. J.; Radom, L.; Schleyer, P. v. R.; Pople, J. A. *Ab initio Molecular Orbital Theory*; Wiley: New York, 1986.
(20) (a) Schlegel, H. B. *J. Comput. Chem.* **1982**, *3*, 214–218. (b) Schlegel, H. B. In *Modern Electronic Structure Theory*; Yarkony, D. R., Ed.; World Scientific Publishing: Singapore, 1994.
(21) Fukui, K. *J. Phys. Chem.* **1970**, *74*, 4161–4163.
(22) (a) González, C.; Schlegel, H. B. *J. Phys. Chem.* **1990**, *94*, 5523–5527. (b) González, C.; Schlegel, H. B. *J. Chem. Phys.* **1991**, *95*, 5853–5860.
(23) Scott, A. P.; Radom, L. *J. Phys. Chem.* **1996**, *100*, 16502–16513.
(24) (a) Reed, A. E.; Weinstock, R. B.; Weinhold, F. *J. Chem. Phys.* **1985**, *83*, 735–746. (b) Reed, A. E.; Curtiss, L. A.; Weinhold, F. *Chem. Rev.* **1988**, *88*, 899–926.
(25) Noury, S.; Krokidis, X.; Fuster, F.; Silvi, B. *Comput. Chem.* **1999**, *23*, 597–604.

TABLE 1. B3LYP/6-31G* Relative[a] Enthalpies (ΔH in kcal/mol), Free Energies (ΔG in kcal/mol), and Entropies (ΔS in cal/(mol K)), Computed at 353.15 K and 1 atm, for the Stationary Points Involved in the Domino Reactions between the OQC 22 and TME 24

	ΔH, kcal/mol	ΔG, kcal/mol	ΔS, cal/(mol·K)
TS1	28.1	26.8	3.7
23	24.2	21.4	7.9
TS2	28.9	43.6	−41.5
25	−41.7	−22.3	−55.1

[a]Relative to **22** and **24**.

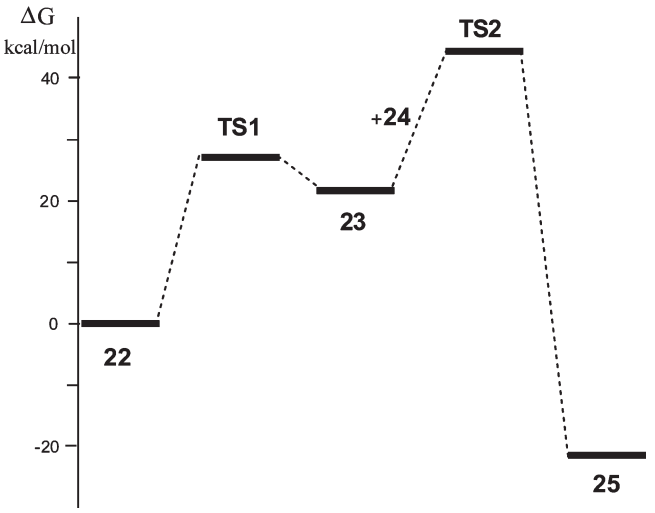

FIGURE 1. Free energy profile (in kcal/mol) for the domino reaction of the OQC **22** with TME **24**.

are in reasonable agreement with the high temperature required for the reaction (80−100 °C).[16] However, the high exergonic character of the overall domino reaction makes this reaction feasible (see later).

The subsequent intermolecular 32CA reaction between the CY **23** and TME **24** takes place through a synchronous concerted bond formation process. The activation energy associated with the concerted **TS2** is very low, 4.7 kcal/mol; the intermolecular 32CA reaction is strongly exothermic, −65.9 kcal/mol. The high exothermic character of this step makes the overall reaction exothermic by −41.7 kcal/mol. Similar kinetic and thermodynamic parameters were obtained for the nonpolar 32CA reaction between the simplest AY **8** and ethylene **2**.[6]

As the two 32CA reactions involved in this domino process present unlike molecularity, the free energies were computed at 80 °C. A schematic representation of the free energy profile is shown in Figure 1. The inclusion of the thermal corrections and entropies to the energies slightly decreases the unfavorable relative free energies associated with **TS1** and CY **23**, in part due to the slight increase of the entropies. However, this factor together with the high reaction temperature disfavors the subsequent intermolecular 32CA reaction, locating **TS2** over **TS1** on the free energy surface. Consequently, the intermolecular 32CA reaction is the rate-determining step of the domino reaction. The free activation energy associated with this domino process is very high, 43.6 kcal/mol.

However, the high exergonic character of the intermolecular 32CA reaction, −65.9 kcal/mol, preserves the exergonic character (−22.3 kcal/mol) of the overall domino process. Consequently, this thermodynamic parameter can

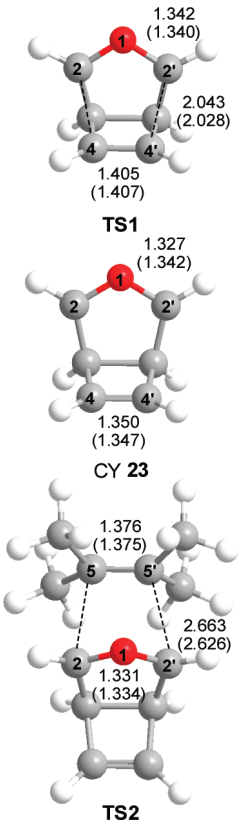

FIGURE 2. B3LYP/6-31G(d) geometries of **TS1** and **TS2** and the intermediate CY **23** associated with the domino reaction of the OQC **22** with TME **24**. The lengths are given in angstroms. The B3LYP/6-311G(d,p) parameters are given in parentheses.

be considered the driving force of the reaction between OQC **22** and TME **24**.

The geometries of the TSs and the intermediate CY **23** are given in Figure 2. A comparison of the B3LYP/6-31G(d) and B3LYP/6-311G(d,p) geometries shows that there are no significant differences. At the **TS1**, associated with the intramolecular retro-32CA reaction, the length of the C2−C4 breaking bond is 2.043 Å, while the O1−C2 bond length is 1.342 Å. The length of the C4−C4′ bond, 1.405 Å, indicates the slight π character of this C−C bond. At **TS2**, associated with the intermolecular 32CA reaction, the length of the C2−C5 forming bonds is 2.663 Å, while the O1−C2 and C5−C5′ bond lengths are 1.331 and 1.376 Å, respectively.

The extent of the bond-formation at the TSs is provided by the bond order (BO).[26] At the **TS1**, the BO value of the C2−C4 breaking bonds is 0.45, while the O1−C2 and C4−C4′ BO values are 1.08 and 1.42, respectively. The last value points to some π character at the C4−C4′ bond, as indicated at the geometrical analysis (see above). At **TS2**, the BO value of the C2−C5 forming bond is 0.17, while the O1−C2 and C5−C5′ BO values are 1.12 and 1.65 respectively. Both the geometrical parameters and the BO values indicate that **TS2** is very early in clear agreement with the low activation barrier and the highly exothermic character of the process.[27]

(26) Wiberg, K. B. *Tetrahedron* **1968**, *24*, 1083–1096.
(27) Hammond, G. S. *J. Am. Chem. Soc.* **1955**, *77*, 334–338.

The electronic nature of the intermolecular 32CA reaction between CY **23** and TME **24** was also evaluated by performing a natural population analysis (NPA) at **TS2**. At this TS, the natural charge at the CY fragment is +0.05 e. Therefore, there is an unappreciable CT from the CY **23** to the TME moiety. This low CT is in complete agreement with the reactivity indices of the CY **23**: $\omega = 0.83$ and $N = 4.94$ eV, and TME **24**: $\omega = 0.43$ and $N = 3.19$ eV. In spite of the large nucleophilic character of the CY **23**, the unappreciable electrophilic character of TME **24** prevents any polar interaction.

The nonpolar character of the intermolecular 32CA reaction between CY **23** and TME **24** is also supported by the very low dipole moment of the species involved in the intermolecular 32CA reaction: CY **23** (0.27 D), TME **24** (0.00 D), **TS2** (0.53 D), and CA **25** (1.42 D). Therefore, it is be expected that solvent effects will have negligible incidence on the gas phase energies and geometries.

3.2. Geometrical and Electronic Structure Analysis of the CY 23. The most relevant geometric and electronic parameters of the CY **23** are given in Figure 2. The lengths of the O1−C2 bonds are 1.327 Å, while the corresponding BO values are 1.15. Additionally, the lengths of the C2−C3, C3−C4, C3−C3′, and C4−C4′ bonds are 1.487, 1.520, 1.629, and 1.350 Å, respectively, while the corresponding BOs values are 1.05, 0.99, 0.93, and 1.81, respectively. These parameters show that while the O1−C2 bonds have a slight π character, the C4−C4′ bond is a double bond.

To achieve a better understanding of the electronic structure of CY **23**, the most relevant molecular orbitals (MOs) were analyzed. These MOs are depicted in Figure 3. The MO 25 of CY **23**, which corresponds to the HOMO, is a nonbonding n MO with a p_z symmetry and with a nodal plane at the oxygen atom. The electron density of this full occupied nonbonding MO is mainly symmetrically distributed at the C2 and C2′ carbon atoms (see the shape of MO 25 in Figure 3). This behavior is responsible for the pseudoradical character of CY **23**.[6,8]

MO 24 has a π bonding symmetry with the electron density mainly located between the C4 and the C4′ atoms. This MO is associated with the π bond of the C4−C4′ double bond. MOs 19 to 23 have a σ symmetry, and they do not participate in the 32CA reaction.

MO 18, which is almost entirely located at the C2−O1−C2′ framework, also presents a π bonding symmetry, and is mainly extended at these three atoms. This MO may be associated with one of the two lone pairs of the O1 oxygen atom. The large delocalization of this MO is responsible for its larger stabilization, and it accounts for the slight π character of the O1−C2 bond.

Three Lewis structures can be drawn for the CY **23** (see Chart 1). While structure **I** corresponds with a diradical structure, structures **II** and **III** have a zwitterionic nature. Organic chemists usually employ structures **II** or **III** to represent the CY as dipoles. Taking into account the analysis of the MOs depicted in Figure 3, one can see that the shape of the nonbonding n MO 25 can be related to diradical Lewis structure **I**. On the other hand, π MO 18 can be related to a resonant structure between **II** and **III**, in which one of the lone pairs of the oxygen is delocalized over C2 and C2′ carbon atoms. Note that Szeimies et al. represented the CY **20** with the Lewis structures **II** and **III** (see Scheme 4).[14]

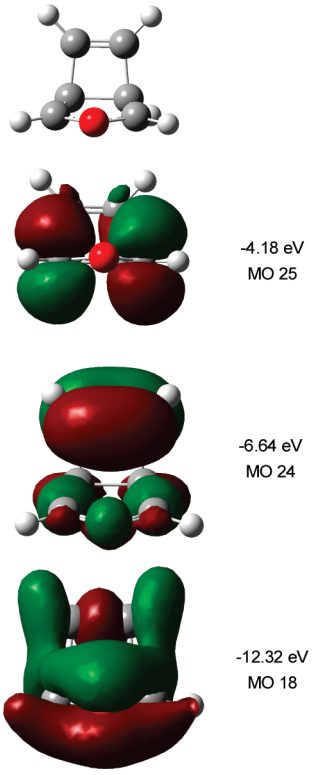

FIGURE 3. Relevant MOs at the B3LYP/6-31G(d) level of theory for CY **23**.

CHART 1. Lewis Structures of the Carbonyl Ylide 23

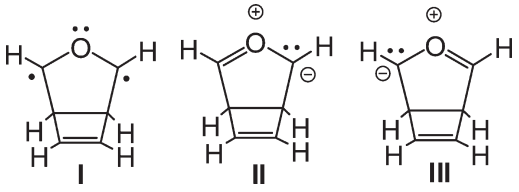

3.3. ELF Analysis of the Bond-Formation Process along the Intermolecular 32CA Reaction between CY 23 and TME 24. Recent theoretical studies have shown that the topological analysis of the ELF along the reaction path associated with a cycloaddition is a valuable tool to understand the bonding changes along the reaction.[6,28,29] The characterization of electron delocalization and the bonding pattern associated to the most relevant points of the reaction pathway would allow us to gain an insight into the electronic reorganization along this 32CA reaction.[6,10,11] With this purpose, the valence basin populations of different geometries taken from the IRC of the reaction between CY **23** and TME **24**, characterized by the C2−C5 distance (D), have been collected and analyzed. The population of the most relevant valence

(28) (a) Berski, S.; Andres, J.; Silvi, B.; Domingo, L. R. *J. Phys. Chem. A* **2003**, *107*, 6014–6024. (b) Polo, V.; Andres, J.; Castillo, R.; Berski, S.; Silvi, B. *Chem.—Eur. J.* **2004**, *10*, 5165–5172. (c) Domingo, L. R.; Picher, M. T.; Arroyo, P.; Saez, J. A. *J. Org. Chem.* **2006**, *71*, 9319–9330. (d) Berski, S.; Andres, J.; Silvi, B.; Domingo, L. R. *J. Phys. Chem. A* **2006**, *110*, 13939–13947. (e) Polo, V.; Andres, J.; Berski, S.; Domingo, L. R.; Silvi, B. *J. Phys. Chem. A* **2008**, *112*, 7128–7136.

(29) Domingo, L. R.; Chamorro, E.; Pérez, P., *Org. Biomol. Chem.* **2010**, *8*, 5495−5504.

TABLE 2. ELF Basin Populations of Selected Points of the IRC of the Intermolecular 32CA Reaction of CY 23 with TME 24[a]

basins	CY **23** and TME **24**	D = 3.48	D = 2.66, **TS2**	D = 2.41	D = 2.18	D = 1.98	D = 1.57, CA **25**
V(O1)	3.58	3.59	3.87	4.26	4.56	2.72	2.52
V′(O1)						2.11	2.62
V(O1−C2)	1.82	1.82	1.76	1.60	1.46	1.32	1.20
V(O1−C2′)	1.82	1.83	1.76	1.60	1.46	1.33	1.20
V(C2)	0.54	0.59	0.82	0.91			
V′(C2)	0.47	0.43					
V(C2′)	0.54	0.59	0.82	0.91			
V′(C2′)	0.48	0.43					
V(C2−C5)					1.00	1.77	1.96
V(C2′−C5′)					1.00	1.77	1.96
V(C5)				0.45	0.64		
V(C5′)				0.45	0.64		
V(C5−C5′)	1.81	1.87	3.67	2.75	2.35	2.14	1.93
V(C5−C5′)	1.95	1.86					

[a]See text for details.

basins of the selected points on the IRC is depicted in Table 2, while ELF isosurface pictures for **TS2** and the IRC point with $D = 2.41$ Å are represented in Figure 4.

The ELF picture of the bonding of the isolated CY **23** reveals four monosynaptic basins, a pair on C2 and another one on C2′ (e.g., V(C2) and V′(C2); V(C2′) and V′(C2′)). The integration of the electronic density in each of these regions corresponds to 0.54 e (V(C2) and V(C2′)) and to 0.47 e (V′(C2) and (V′(C2′)); see Table 2), providing a bonding structure picture where 1.01 e is located on each terminal carbon. This picture agrees qualitatively with the electronic density displayed by MO 25 of CY **23** (see Figure 3) and is responsible for the pseudodiradical behavior of CY **23**. Additionally, each of the V(O1−C2) and V(O1−C2′) disynaptic basins associated to the C−O bond regions integrates 1.82 e, a higher electronic density than that at the OQC **22**, where these regions integrate 1.30 e. The oxygen O1 has a monosynaptic basin that integrates 3.58 e; this value is lower than that at OQC **22**, 4.88 e. Therefore, there is a partial delocalization of electron density of one of the oxygen lone pairs over the O1−C2 and O1−C2′ bond regions (see MO 18 in Figure 3). A similar ELF picture is found for the open shell wave function of CY **23** (see the Supporting Information). The more relevant changes in the electronic density of the open shell wave function of CY **23** are as follows: (i) the two monosynaptic basins present at C2 and C2′ terminal carbons are merged in a unique monosynaptic basin that integrate 0.74 e each, and (ii) while the population of the V(O1−C2) and V(O1−C2′) disynaptic basins decreases to 1.70 e, the population of the V(O1) monosynaptic basin increases to 3.82 e. These changes in electronic density do not modify the chemical behavior of CY **23**. This electronic picture is similar to that found at the simplest AY **8**.[6] At this point, the bonding at the CY **23** resembles the diradical Lewis structure **I** depicted in Chart 1, and it accounts for the pseudodiradical chemical behavior of CY **23**.

Analyzing now the valence basin populations of different geometries taken from the IRC of the reaction between CY **23** and TME **24**, characterized by the C2−C5 distance (D), we can see that, as the two reactants (CY **23** and TME **24**) approach each other toward the TS region ($3.86 < D < 2.66$ Å), the main electronic reorganization occurs on the CY **23** side, whereas TME **24** remains almost unchanged. In this way, isolated TME **24** has two disynaptic basins, V(C5−C5′) and V′(C5−C5′), with 1.81 and 1.95 e, respectively, which merge at **TS2** ($D = 2.66$ Å) into one V(C5−C5′) integrating 3.67 e. Meanwhile, at CY **23** moiety, the two monosynaptic basins over C2 and C2′ merge into one at **TS2** with a smaller electronic integration (see Table 2) providing a bonding structure picture where 0.82 e are located on each ylide terminal carbon. Note that on going to **TS2** there is a flux of the electron density from the V′(C2) and V′(C2′) basins to the V(C2) and V(C2′) ones until reaching **TS2**, where the V′(C2) and V′(C2′) basins disappear.

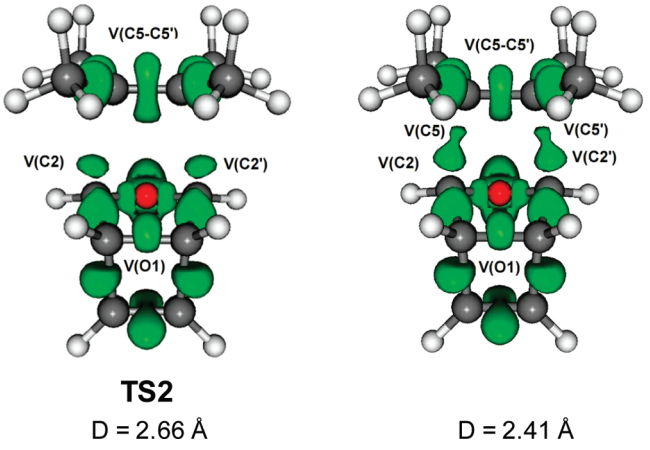

FIGURE 4. ELF isosurface pictures for **TS2** and the IRC point of $D = 2.41$ Å.

After passing the **TS2** region ($D < 2.66$ Å), the two monosynaptic regions (e.g., V(C2) and V(C2′) basins) increase their electronic population to 0.91 e ($D = 2.41$ Å) whereas at TME **24** two new monosynaptic regions over each carbon of the ethylene moiety (V(C5) and V(C5′)) appear with an electronic integration of 0.45 e, coming from the decrease of the electronic integration of the V(C5−C5′) disynaptic basin (see structure $D = 2.41$ Å in Figure 4).

At $D = 2.18$ Å, the monosynaptic basins over the terminal carbons at the CY moiety, C2 and C2′, are converted into disynaptic ones (V(C2−C5) and V(C2′−C5′)) with an electronic integration of 1.00 e, verifying the formation of the new bonds between C2−C5 and C2′−C5′ at this distance. At this point on the IRC, the monosynaptic basins on the ethylenic carbon atoms of TME **24** (V(C5) and V(C5′)) increase their electronic integration to 0.64 e but at $D = 1.98$ Å the electronic integration of these basins is incorporated into the disynaptic bond basins V(C2−C5) and V(C2′−C5′), with 1.77 e each.

The electronic population of these basins increases now from 1.77 e at 1.98 Å to 1.96 e at 1.57 Å (CA **25**).

Very recently, we have reported that the unfavorable π electron-reorganization demanded in the nonpolar DA reaction between cyclopentadiene **1** and ethylene **2** to reach pseudodiradical species involved in the concerted C−C bond formation is responsible for the high activation energy, 19.9 kcal/mol (see Scheme 1).[29] Now, the pseudodiradical character of CY **23**, which is preserved at **TS2**, accounts for the very low activation energy associated with this nonpolar 32CA reaction, and for the earlier (more reactant-like) character of the TS (see **TS2** in Figure 4). This finding offers a sound explanation of the high reactivity of AY **8** toward ethylene **2** found by Hiberty et al.,[15] which was attributed to the "diradical" character of AY **8** and the corresponding TS.

It is noteworthy to detail the evolution of the electron density of the lone pairs at the O1 oxygen atom along this nonpolar 32CA process. The ELF of the CY **23** indicates that the O1 oxygen atom has only one monosynaptic basin V(O1) that integrates 3.58 e. This basin accounts for the two lone pairs on the O1 oxygen atom. The loss of ca. 0.4 e of electronic density on the V(O1) oxygen basin can be related to some electronic delocation on the neighboring C2 and C2′ carbon atoms, which is advanced by the shape of MO 18 of CY **25** (see Figure 3). Along the IRC, the population of the V(O1) basin increases, while the population of the disynaptic basins V(O1−C2) and V(O1−C2′) decreases. This behavior is more evident after passing **TS2** (D < 2.66 Å), where two new disynaptic basins V(C2−C5) and V(C2−C5′) are created (D = 2.18 Å) and the V(O1) basin is split into two new monosynaptic basins: V(O1) and V′(O1) (D = 1.98 Å, see Table 2). Consequently, ELF analysis suggests that along the 32CA reaction the two oxygen lone pairs are mainly located on the CY oxygen atom, and hence, they do not participate along the C−C bond formation.

Therefore, this topological analysis of the ELF, which is similar to that for the nonpolar 32CA reaction between the simplest AY **8** and ethylene **2**, provides further support to the concept of regarding this 32CA process as a result of a concerted attack of two nonbonding electrons, each one located at the terminal carbon atoms of the CY fragment, over the π system of the ethylene derivative, which is activated toward the attack of the ylide pseudoradical carbon atoms only after the TS region has been reached. Therefore, the interaction between CY **23** and TME **24** takes place at long distances, once the TS region has been passed at D < 2.66 Å. The electronic structure of the CY **23** based on the MO analysis and the population analysis based on the topological analysis of the ELF reveals that the pseudodiradical character of CY **23** and AY **8** provides the electronic activation of the nonactivated ethylene derivatives.[6]

According to ELF analysis, the interaction between CY **23** and AY **8** with nonactivated ethylenes, which does not show a pericyclic electron reorganization, should be classified as a [2n + 2π] processes. Note that the oxygen and nitrogen lone pairs of these three-atom components of 32CA reactions do not participate in the C−C bond formation.

4. Concluding Remarks

The thermal addition of TME **24** to the OQC **22** has been studied by using DFT methods at the B3LYP/6-31G* level. This reaction is a domino process that comprises two consecutive 32CA reactions: an intramolecular retro-32CA reaction at the OQC **22** to yield CY **23**, which experiences a subsequent intermolecular 32CA reaction toward TME **24** to afford the final CA **25**. The high activation energy associated with the first retro-32CA reaction together with the unfavorable activation entropy associated with the second intermolecular process cause the global process to display high free activation energy. This fact justifies the high temperature demanded in these thermal processes. However, the highly exothermic process associated with these 32CA reactions, together with the loss of the strain on the OQC **22** make these domino processes strongly exergonic. Therefore, these reactions are thermodynamically controlled.

The electronic structure of the CY **23** based on the MO analysis and the topological analysis of the ELF along the intermolecular 32 CA reaction of the CY **23** and TME **24** provide a new scope of the electronic structure of CY **23** as a pseudodiradical species offering a sound explanation of the high reactivity of the CYs. In addition, this analysis points to the nonparticipation of the oxygen lone pairs in the 32CA reaction. This cycloaddition can be seen as a "pseudodiradical attack" of the terminal carbon atoms of the CY **23** on the π system of TME **25**. Therefore, the present study establishes that this nonpolar 32CA reaction, which is not a pericyclic electron reorganization, may be electronically classified as a [2n + 2π] process.

Acknowledgment. Financial support from the MICINN (Project CTQ2009-11027/BQU) is acknowledged.

Supporting Information Available: B3LYP/6-31G* and B3LYP/6-311G** total and relative energies for the stationary points involved in the domino reaction between the OQC **22** and TME **24**, B3LYP/6-31G* enthalpies, free energies, and entropies for the stationary points involved in the domino reaction between the OQC **22** and TME **24**, UB3LYP/6-31G(d) geometry and ELF basin populations of CY **23**, complete citation for ref 17, and B3LYP/6-31G* and B3LYP/6-311G** computed total energies, unique frequency imaginary, and Cartesian coordinates of the stationary points involved in the domino reaction between the OQC **22** and TME **24**. This material is available free of charge via the Internet at http://pubs.acs.org.